PCCP

ROYAL SOCIETY OF CHEMISTRY

PERSPECTIVE

View Article Online
View Journal | View Issue

Cite this: *Phys. Chem. Chem. Phys.*, 2021, **23**, 9049

Substance and shadow of formamidinium lead triiodide based solar cells

Muhammed P. U. Haris,[a] Samrana Kazim,[ab] Meenakshi Pegu,[a] M. Deepa[c] and Shahzada Ahmad *[ab]

Received 5th February 2021,
Accepted 16th March 2021

DOI: 10.1039/d1cp00552a

rsc.li/pccp

The current decade has witnessed a surge of progress in the investigation of methyl ammonium lead iodide ($MAPbI_3$) perovskites for solar cell fabrication due to their intriguing electro-optical properties, despite the intrinsic degradation of the material that has restricted its commercialisation. As a promising alternative, solar cells based on its formamidinium analogue, $FAPbI_3$, are currently being actively pursued for having demonstrated a certified efficiency of 24.4%, while the room-temperature conversion to a non-perovskite δ-phase impedes its further commercialisation, and strategies have been adopted to overcome this phase instability. An in-depth and real-time understanding of microstructural relationships with optoelectronic properties and their underlying mechanisms using operando *in situ* spectroscopic techniques is paramount. Thus, the design and development of a new process, data driven methodology, characterization and evaluation protocols for perovskite absorber layers and the fabricated devices is a judicious research direction. Here, in this perspective, we shed light on the compositional, surface engineering and crystallization kinetics manipulations for $FAPbI_3$, followed by a proposition for unified testing protocols, for scalling of devices from the lab to the market.

1. Introduction

In an era where greenhouse gas emission is showing a steep rise and carbon neutral technology is sought after,[1] photovoltaic (PV) deployment is gaining momentum as a green and clean source of energy. PV technology is suited to fulfil the growing energy demand by being cost effective and has demonstrated grid parity in parts of the world. To cater to the planet's demand and large-scale deployment, thin film PV technology other than that of Si is being investigated.[2] Thin film PV devices equipped with added functionalities, such as the prospect of being lightweight and cost competitive, make them strong contenders for future portable and utility scale applications. In recent years, the investigation of hybrid inorganic–organic halide perovskites (Fig. 1a) for solar cell

[a] *BCMaterials, Basque Center for Materials, Applications and Nanostructures, UPV/EHU Science Park, 48940 Leioa, Spain. E-mail: shahzada.ahmad@bcmaterials.net; Tel: +34 946128811*
[b] *IKERBASQUE, Basque Foundation for Science, Bilbao, 48009, Spain*
[c] *Dept. of Chemistry, IIT Hyderabad, Kandi, Sangareddy-502285, Telangana, India*

Muhammed P. U. Haris

Muhammed P. U. Haris obtained his bachelor degree in chemistry from University of Calicut (Kerala), India, in 2015 and his MSc degree in chemistry from Mahatma Gandhi University Kerala, India, in 2017. He then worked at National Chemical laboratory. Currently, he is pursuing his doctorate degree under Prof. Shahzada Ahmad. His research interest is focused on the synthesis and characterization of halide perovskite materials and their photovoltaic applications.

Samrana Kazim

Samrana Kazim is Ikerbasque fellow and a group leader. Prior to this, she has worked as a tenured Senior scientist (2013–2017) at a corporate research center of Abengoa. Her current research is focused on Designing, synthesis, and characterization of nanostructured materials, hybrid inorganic–organic solar cells, and charge transport properties of organic semiconductor.

fabrication has gained significant attention owing to their high solar-to-electric conversion efficiencies at the lab scale, low-precursor cost of materials and ability for solution processability.[3,4] The reported power conversion efficiency (PCE) is on par with the mature PV technology and has reached beyond 25%, which is also suited for self-powered internet of things based devices[5] or utility scale applications. Among the materials for the emerging thin film PV technology, perovskites supersede others in terms of performance (Fig. 1b). Perovskites are known for over a century; however, their application for solar cells was exploited a decade ago and it turned out to be a game changer in PV research. The extremely high absorption coefficient of semiconducting perovskites and their intriguing opto-electrical properties enable perovskites to be efficient light harvesters, and arguably less than a micrometre (300–500 nm) thick perovskite layer can harvest the same amount of light as effectively as a thick silicon (200–300 μm) wafer does. Typically, a perovskite solar cell (PSC) is a thin film device consisting of a transparent conducting oxide as the charge collector, a perovskite as the light harvester and charge selective layers as efficient charge extractors (Fig. 1c). Both mesoscopic and planar (n–i–p) architectures are being fabricated (Fig. 1c), while inverted planar (p–i–n) structures have also been reported, where moderate heat treatment for a hole selective layer is not an issue. Upon light irradiation, electron–hole pairs are created in the absorber layer, which dissociate and transport to their respective charge selective layers, *i.e.*, the electrons travel to the electron transport layer (ETL), while the positive charge (holes) travels to

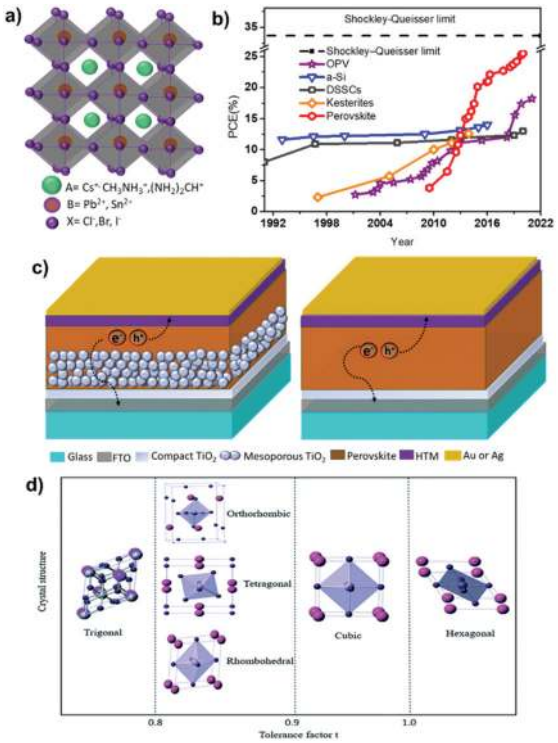

Fig. 1 (a) Structure of alkylammonium halide perovskites, (b) certified efficiencies of emerging thin film photovoltaics, (c) mesoscopic and planar (n–i–p) perovskite solar cell architectures and (d) relation between the perovskite crystal structure and tolerance factor. Reproduced with permission from ref. 9 copyright 2019, Royal Society of Chemistry.

Meenakshi Pegu

Meenakshi Pegu has received her Master Degree in Chemical Sciences from Indian Institute of Technology, Guwahati, India. She then joined Indian Institute of Science (Bangalore) as a research assistant to work in a Ministry of Science and Technology funded project. She is currently working towards her doctorate degree in the group of Prof. Shahzada Ahmad. Her research work is primarily focused on the arena to develop and synthesize new novel hole transporting materials, interface engineering of perovskite layer with organic molecules for device stability, developing new bilayer perovskites and studying the interactions.

M. Deepa

Melepurath Deepa received her PhD from Delhi University in 2004. She is currently a Professor of Chemistry at Indian Institute of Technology (IIT Hyderabad), India. Her research interests include developing materials and novel design architectures for solution processed solar cells, and their application to dual function devices like photo-supercapacitors and photoelectrochromic cells.

Shahzada Ahmad

Shahzada Ahmad is Ikerbasque professor; his scientific interests include materials for energy applications. His research spans across the fields of physical chemistry, nanotechnology and materials science with a view to developing advanced materials for energy application and unraveling device kinetics. He enjoys fusion cooking.

the hole transport layer (HTL); thus, the collected charge carriers at the FTO and metal electrode generate photocurrent at the outer circuit.

The structure and optoelectronic properties of halide perovskite are well studied and we direct the readers to the reviews.[6,7] It is imperative to confine the structural and optoelectronic credentials of halide perovskites within a range for its implementation in PSCs. Importantly, the structural stability of ABX_3 perovskite is determined using the Goldschmidt tolerance factor (t) and is represented by the formula,

$$t = (r_A + r_X)/(\sqrt{2}(r_B + r_X)$$

where r_A, r_B and r_X represent the ionic radii of A, B and X, respectively. Arguably, the value of $0.9 \leq t \leq 1$ is the ideal tolerance factor range to form the cubic perovskite structure. It can be deduced from Fig. 1d that any deviation from this range will lead to structural distortion and unfavourable phase transition.[8,9]

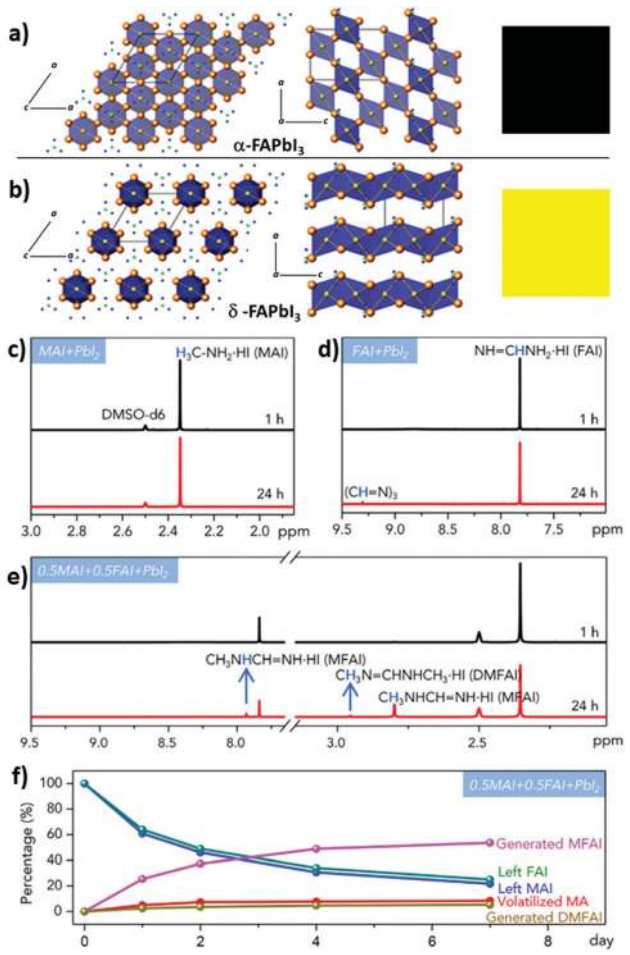

Fig. 2 (a and b) Polyhedral representations of the black (a) and yellow (b) polymorphs of $FAPbI_3$. The blue polyhedra represent the PbI_6 octahedra, with the Pb and I atoms shown as yellow and orange spheres, respectively. Reproduced with permission from ref. 32 copyright 2014 American Chemical Society. (c–e) ^{1}H NMR spectra of different perovskite precursor solutions with aging and (f) compositional evaluation from the ^{1}H NMR data. Reproduced with permission (d–f) from ref. 36 Copyright 2020 Elsevier.

Moreover, the intrinsic and extrinsic degradation pathways prevalent in PSCs have plagued its commercial endeavour. Plausibly, in the case of the widely exploited $MAPbI_3$ (methyl ammonium lead iodide), the volatile nature of the organic cation, halide segregation and crystal size expansion are undesirable processes that accelerate device degradation.[10] Ions have the natural tendency to move, an undesirable process that promotes various types of recombination losses in the fabricated PSCs.[11] Studies reviled that such degradations induced further defects, which limit the long-term stability of the device.[10–13]

Baikie and co-workers introduced a perovskite with broader absorption and an improved thermodynamic stability.[14] The replacement of the MA cation by a larger Formamidinium (FA) cation maintained the ABX_3 symmetry with a large t value which eventually reduced the band-gap to $\sim$1.47 eV closer to the optimum value of $\sim$1.4 eV. In a parallel work, Snaith *et al.* reported a champion PCE of 14.2% and suggested $FAPbI_3$ as the future alternative for the degradation prone $MAPbI_3$.[15] However, the X-ray and neutron powder diffraction studies of $FAPbI_3$ reported the existence of two polymorphs, a black photoactive-perovskite material with a cubic symmetry (α-phase) and a yellow non-perovskite (δ-phase) hexagonal photo-inactive counterpart (Fig. 2a and b). In contrast to $MAPbI_3$, a phase transition from α to δ-phase takes place upon moisture exposure at low temperatures. Although it lacks the detailed understanding of factors affecting the degradation dynamics of $FAPbI_3$, the thermal decomposition studies on powder $FAPbI_3$ revealed the formation of 1,3,5-triazine (*s*-triazine), hydrocyanic acid, and ammonia at 95 °C[16] as depicted in Scheme 1.

Recent studies suggest that the intrinsic lattice strain and extrinsic induced strain such as thermal expansion coefficient are a mismatch between the perovskite and the substrate. Disparity in the local lattice at the perovskite interface and crystal phase in doped perovskites has deleterious effects on the optoelectronic properties of perovskite caused by the formation of defects and by dislocation in grains and grain boundaries.[17–21] The produced defects not only accelerate the photo-, heat- and moisture induced chemical degradation but

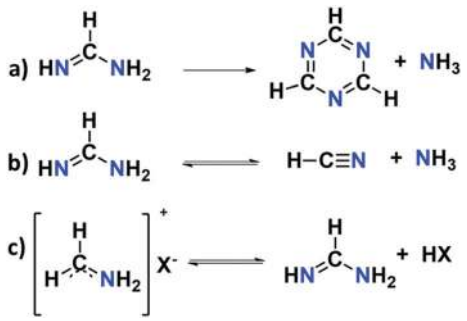

Scheme 1 Thermal decomposition reaction of formamidine generating (a) *s*-triazine and (b) HCN. (c) Reverse of the acid (HX)/base (formamidine) neutralization for the formation of formamidinium halide salt, FAX (X = Br, I). Reproduced with permission from ref. 16 copyright 2019, Royal Society of Chemistry.

also adversely affect the charge carrier mobility, which destabilizes the PSCs.[19–22] In addition to the unfavourable phase transition and thermal degradation, smart strain engineering has also emerged as a challenge to stabilize the $FAPbI_3$, where low defect density and superior charge transportation can be achieved.

To an extent, such adverse processes can be controlled, by the extrinsic doping of perovskites and these interfacial doping agents provide avenues for improvement in PSC performance.[23] The use of such dopants or an additional layer or new crystallization routes protects or curtails the moisture-, heat- and photo-induced damage, induces better charge carrier dynamics and improves the intrinsic structural stability which can synergically boost the PV performance. Studies related to compositional engineering, interfacial modification, charge carrier dynamics and controlled crystallization of metal halide perovskites have been reported.[24–27] In this perspective, we have shed light on the role of compositional engineering, interfacial modifications, controlled crystallization, and deciphering device kinetics on structural stability, charge carrier dynamics and defect engineering for the fabrication of high quality $FAPbI_3$ layers and PSCs thereof. Furthermore, we have extended the discussion to the need of unified testing protocols to foster the commercialisation of PSCs.

2. Road map for $FAPbI_3$ based PSC

2.1 Compositional and dimensional engineering

Compositional engineering of 'A', 'X' and 'B' sites in ABX_3 is an effective pathway to improve the physical and structural properties without significantly altering the optoelectronic properties. Partial substitution by MA, cesium (Cs), rubidium (Rb), bromide (Br), and chloride (Cl) in $FAPbI_3$ or their combinations were well explored and yielded performance and stability enhancement in devices.[28–30] Doping with smaller cations such as MA, Cs and Rb was demonstrated to lower the tolerance factor from 1.04 to the ideal range.[31–33] Initial reports with MA doping formed stable $FAPbI_3$ without any phase segregation at room temperature, where, Bein *et al.* attributed the stabilisation of $FA_xMA_{1-x}PbI_3$ to the higher dipole moment magnitude of MA which creates stronger hydrogen bond interactions with the inorganic cage and optimised the MA content to $<20\%$ of FA.[34] Although the MA content improved the phase stability and efficiency of $FAPbI_3$, the chemical instability of MA cation due to its photo- and thermal sensitivity hindered its employment in PSCs. Akin to $MAPbI_3$, the formation of volatile methylamine through the reversible acid–base decomposition induced the deprotonation of MA cations which is reported in MA doped $FAPbI_3$.[35,36] The ^1H NMR studies on precursor solutions (Fig. 2c–f) demonstrated that only a small amount of volatile methylamine leaves the system and the remaining solution immediately condensates with formamidinium iodide (FAI) to form the unwanted *N*-methyl FAI and *N*,*N*-dimethyl FAI. We can deduce (Fig. 2f) the gradual increase in the *N*-methyl FAI upon aging of the precursor solution.[36] By capitalizing the reported knowledge on the compositional engineering of $MAPbI_3$, Cs, K or Rb amalgamated $FAPbI_3$ along with Br or Cl doping delivered improved device performance at the expense of higher bandgap, though the long-term stability of the device under harsh testing conditions remains unclear. The enhanced photo- and moisture-stabilities demonstrated through smaller Cs amalgamation into $FAPbI_3$ opened a new pathway whereby they demonstrated the contraction of the cubo-octahedral volume (Fig. 3a) and a reduction of trap density (Fig. 3b) by an order of magnitude, subsequently increasing the open circuit voltage (V_{OC}) and the fill factor (FF), leading to PCE and stability hike.[37] The inclusion of Cs motivated the researchers to expand the cationic dopant pool with Rb and K, and although this improves the device performance marginally, only Cs displays structural incorporation.[38] Various methodologies were adopted for Cs amalgamation and $>20\%$ of PCE was reported.[39] The understanding of the mechanisms and dynamics with Cs inclusion is of significant interest. The microscopic understanding of structural energy landscape revealed that higher entropy contribution from an organic cation reduces the Gibbs free energy thereby assisting in circumventing phase transitions. FA cation in $FAPbI_3$ is reported to have an isotropic orientation with a large entropy at higher temperatures and upon cooling to room temperature it

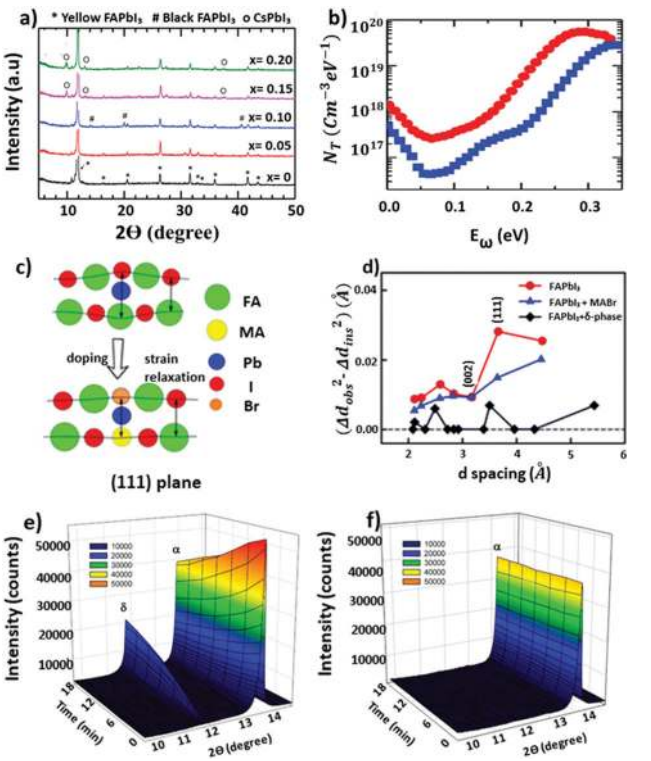

Fig. 3 (a) X-ray diffraction (XRD) patterns of the $FA_{1-x}Cs_xPbI_3$ films, (b) calculated trap density for $FAPbI_3$ (red) and $FA_{0.9}Cs_{0.1}PbI_3$ (blue) perovskite solar cells. (a and b) Reproduced with permission from ref. 47 Copyright 2015, Wiley. (c) Schematic representation of strain relaxation of the (111) plane after MABr alloying, (d) Williamson–Hall plot extracted from diffraction profiles and (e and f) time-dependent XRD measurements of (e) $FAPbI_3$ with phase transition and (f) stabilized $FAPbI_3$–MABr without phase transition under a humid atmosphere with an RH of $\sim$50% at 23 °C. (c–f) Reproduced with permission from ref. 46. Copyright 2016 American Chemical Society.

adopts a strong preferential orientation with a lower entropy.[40] The enhanced entropy upon Cs inclusion contributes to stabilize the perovskite phase at lower temperatures and the Cs concentration has been optimized to 3–20% to balance the bandgap widening and the increase of density of states (DOS) below the valence band maxima (VBM).[41] In addition to the phase stability, different imaging or mapping techniques, such as Synchrotron-based nanoscale X-ray fluorescence (n-XRF),[42] photoluminescence (PL), and hyperspectral imaging,[43] showed that inorganic Cs doping homogenizes the halide distribution between Cl, I and Br and reduces the heterogeneity in the charge carrier dynamics[42,43] which eventually highlighted the ability of the triple-cation-mixed halide perovskites to function as capable light harvesters. The addition of dopants as additives in the precursor solution, a non-uniform distribution at the perovskite surface and bulk has been reported in thin films which significantly affects the structural, optoelectronic and device properties.[44,45] The impact of dopant at the grain and grain boundaries was studied on device performance; understanding of dopant distribution and the effects at the $FAPbI_3$ surface and bulk is paramount for further optimisation.

As discussed in the previous section, the intrinsic lattice strain is detrimental to the successful working of PSCs and this stems from the twisting and tilting of the PbI_6 octahedra and lattice expansion or contraction. The A or X site doping stabilizes the α-$FAPbI_3$ phase at the expense of lattice expansion or contraction which eventually generates the residual strain and influences the optoelectronic properties. Although strain engineering was initially reported for low dimensional and $MAPbI_3$ perovskites, Kim *et al.* reported a strain relaxation strategy of using smaller and larger cations together as dopants to reduce tensile strain and comprehensive strain in the $FAPbI_3$ lattice.[20] The grazing-incidence wide-angle X-ray scattering (GIWAXS) patterns of $FAPbI_3$ modified with equal mole% of smaller (Cs) cation and larger (methylene diammonium) cation showed a reduction of lattice strain and trap density to deliver an unparalleled device with a PCE of 24.4% through prolonged carrier lifetime and reduced Urbach energy. Additionally, the non-encapsulated devices showed superior thermal stability of retaining >80% of the initial PCE after 1300 h of annealing at 85 °C.[20] In addition to single site doping, co-doping strategies have been introduced to relax the residual strain. The anisotropic strain on the (111) lattice plane of $FAPbI_3$ is reported as the driving force for the phase transition and a co-doping strategy where both the A and X sites get doped with comparatively smaller ions (MA^+, Br^-) which reduced the strain along the (111) plane through lattice shrinkage (Fig. 3c).[46] From the micro-strain (Fig. 3d) calculated using the Williamson–Hall plot, where MABr alloying reduced the strain at the (111) lattice plane of α-$FAPbI_3$, they found that MA contributes more towards the phase stabilization. However, the current limitation to obtain a defect-free strained $FAPbI_3$ or defect rich $FAPbI_3$ without strain restricts the individual study of strain and defects to their relationships.

The usage of long organic spacer cations will help to address parts of the existing stability concerns in PSCs. The low dimensional/layered perovskites (in the scientific literature also referred as 2D or quasi 2D) derived from large organic spacers with high intrinsic and extrinsic structural as well as thermal stabilities will enhance the physico-chemical properties, whereas, its poor charge-transport properties owing to the large quantum well and narrow light absorption ability impede its development. Moreover, the layered perovskite surface is known to induce hydrophobicity and the contact angle measurement with water droplet has been used to probe the same. Layered $FAPbI_3$ perovskite showed higher hydrophobicity than the pristine $FAPbI_3$ surface[48] (Fig. 4a and b). Apparently, the employment of an alternate layer of layered (2D) and conventional (3D) *i.e.*, 2D/3D hybrid perovskites was reported to align the interface in order to maximize charge collection and transportation.[24,25,49,50] The approach of having perpendicular orientation of the layered perovskites atop of the 3D (conventional) perovskite to allow uni-directional charge transport and collection was adopted. This bilayer approach was optimized by structural and interfacial packaging control to maximize light harvesting and induced stability.[51] Researchers focussed on the tuning the opto-electrical and structural properties of layered, bilayer, and layered passivation by manipulating the elemental composition, organic spacer, layer thickness and crystallization routes of MA based system and demonstrated reduced exciton binding energy and improved charge carrier dissociation and conductivity. FA cations with a low band gap were also employed in layered PSCs and a PCE of >19% was achieved.[52] Liu *et al.* showed the superior absorption ability of FA over MA that led to

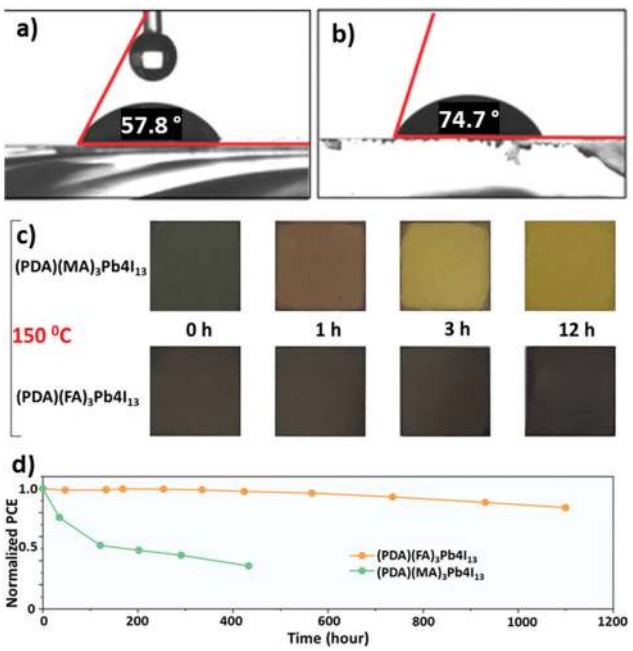

Fig. 4 (a and b) Contact angle measurements of the (a) $FAPbI_3$ and (b) $(PDMA)FA_2Pb_3I_{10}$ perovskite films with a water droplet. (a and b) Reproduced with permission from ref. 48, Copyright 2019 American Chemical Society. (c) Images of the $(PDA)(MA)_3Pb_4I_{13}$ and $(PDA)(FA)_3Pb4I_{13}$ perovskite films taken at various intervals during annealing at 150 °C, (d) thermal stability tests at 85 °C for the corresponding solar cells. Reproduced with permission from ref. 53 Copyright 2021, Wiley.

a high photocurrent and PCE along with superior stability of the layered perovskite over the $FAPbI_3$ under harsh moisture and thermal testing conditions. In another report, Chen *et al.* compared the MA and FA based layered PSCs and $(PDA)(FA)_3Pb_4I_{13}$ demonstrated superior stability. Here, both the perovskites were annealed at 150 °C under N_2 and the digital images were recorded (Fig. 4c). The $(PDA)(MA)_3Pb_4I_{13}$ films turned brown within 1 hour and gradually changed to the non-perovskite (yellow) phase after 3 hours while the FA counterpart showed exceptional stability up to 12 hours of continuous thermal stress. Furthermore, the corresponding PSCs were tested for thermal stability at 85 °C under N_2 atmosphere in dark (Fig. 4d).[53] From the knowledge capitalized from the MA system, it is known that it is vital to focus on the rational selection of organic spacer and crystallization routes to optimize the FA systems. To this end, the employment of an organic spacer with an electron-donating or an electron-with drawing group[54] or hetero-atoms can improve the charge transport. Another approach was to introduce functional donor groups on the cations in order to fine-tune the electrical properties of the layered perovskites. These organic cations can actively participate in the energy band structure of the layered perovskite and in the charge-transfer processes, and subsequently contribute to the optimization of device performance. The incorporation of cations tailored for π–π stacking is imperative for improving the charge-transport properties in low-dimensional perovskites.[55,56] Cations can be tailored to stabilize lead iodide based perovskites through stronger hydrogen bonding coupled with π–π stacking interactions. However, most of the reports on low-dimensional PSCs are restricted to MA cations while the FA cations have rarely been studied and much efforts are needed to elucidate the charge carrier dynamics and thereby boost the PCE for future commercialisation.

2.2 Controlled crystallization

Defects at the grain boundaries and surfaces of polycrystalline perovskite layers are sensitive to moisture and ion migration; these promote intrinsic as well as extrinsic instability of PSCs under operando conditions. Any methodology to decrease the super-saturation of the perovskite solution by increasing the precursor–solvent interactions will limit the nucleation rate and thereby control the defects at grain boundaries. The use of oxygen-, sulphur- and nitrogen-donor Lewis bases/acids with high dipole moment is a well explored methodology to increase the molecular interactions and the nucleation energy barrier to slow down crystallization.[57–59] The choice of non-volatile additives induces uniform layer formation by residing at grain boundaries and passivating charged point defects. In recent years, ionic liquids (ILs) have been employed as non-volatile additives due to their high hydrophobicity, high surface tension properties, low-toxicity and excellent electrochemical properties and among them, the imidazolium based ILs are preferred owing to their high ionic conductivity.[60–65] Enhancement in the PCE of $FAPbI_3$ from 17.1 to 20.06% with a 1-hexyl-3-methylimidazolium iodide (HMII) additive was reported. HMII addition improved the carrier life time from 229 ns to 1382 ns along with an increase in the PL emission suggesting the reduced non-radiative recombination, and authors attributed this to the passivation of vacancies through ionic interactions of HMII.[64] Improved crystallinity and phase purity were observed from morphological and structural analysis. The low trap density of the modified device calculated from space charge limit current (SCLC) measurements supported the crystallinity improvements and reduced non-radiative recombination which resulted in higher V_{oc} and photocurrent. Moreover, HMII enhanced the stability and the device retained 85% of its initial PCE after 250 hours of maximum power point tracking (MPPT) under the ISOS-L-1I protocol. A polymerized ionic liquid (PIL) in a PSC achieved a PCE of 21.4% and an excellent long term operational stability of maintaining 92% of its initial PCE after 1200 hours under 1 sun illumination at 70–75 °C.[66] The synthesized PIL (Fig. 5a) containing multi-anchoring sites forms high quality films with large grains. The authors reported that the PIL species were immobilized at the grain boundaries and passivate the under-coordinated Pb ion defects which eventually resulted in excellent stability under harsh conditions. Although the role of the alkyl chain on the imidazole ring has been well studied, the understanding of the effects of the anionic part and the interactions with $FAPbI_3$ requires further investigation.

Spin coating method followed by an anti-solvent dripping and high temperature (150 °C) annealing is the way to fabricate high quality $FAPbI_3$ layers. The higher thermal expansion coefficient of $FAPbI_3$ over the substrate and the temperature gradient between the bottom and top surface of the $FAPbI_3$ layer upon annealing will induce a large residual strain.[67,68] The faster annealing or expansion at the bottom surface and faster cooling from the top surface of $FAPbI_3$ due to temperature gradient leads to tensile strain on the surface and comprehensive strain in the bulk (Fig. 5c).[69] Moreover, the thermal coefficient gradient between the perovskite and the substrate induces an additional tensile strain to the bulk eventually

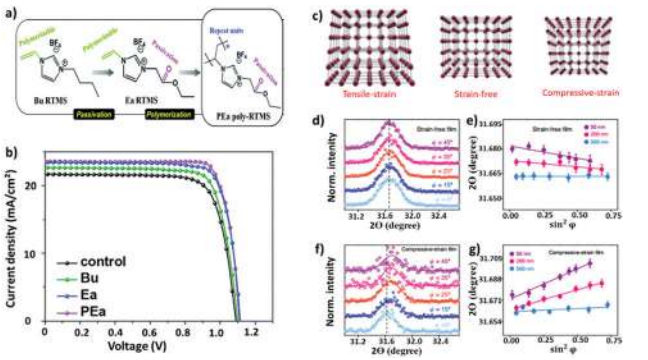

Fig. 5 (a) Schematic representation of ILs and PIL, (b) J–V characteristics of devices with modified perovskite absorbers. (a and b) Reproduced with permission from ref. 66, copyright 2020, Royal Society of Chemistry. (c) Schematic representation of different strain states at the perovskite surface, (d and f) GIXRD spectrum at different tilt angles at a depth of 50 nm for the strain-free film and the compressive strained film. (e and g) Residual strain distribution at depths of 50, 200, and 500 nm for the strain-free film, compressive strained film (measured (points) and Gauss fitted (line) diffraction strain data as a function of $\sin 2\theta$). The error bar indicates standard deviation of 2θ. (c–g) Reproduced with permission from ref. 69 copyright 2019, Springer Nature.

leading to a gradient residual strain in the perovskite layer that affects the optoelectronic properties. A protocol to minimize the gradient residual tensile strain of the perovskite layer using a flipping method, where the spin coated perovskite is annealed from the perovskite surface instead of the substrate surface, has been introduced.[69] The residual strain distribution was calculated from grazing incident X-ray diffraction (GIXRD) measurement (Fig. 5d and f) for pristine and flipped thin films where a smaller strain gradient was visible for the film fabricated through flipping method. The detailed analysis of strain distribution across the film thickness showed homogeneous lattice parameter for the flipped film and a vertical gradient lattice structure for the pristine film as depicted in Fig. 5g and e, respectively. To this end, it is crucial to design effective strategies to reduce the annealing temperature of the $FAPbI_3$ film and to introduce new substrate materials with thermal coefficients similar to that of $FAPbI_3$ which could synergically lower the temperature and strain gradients, throughout the perovskite layer.

2.3 Interfacial engineering

Optimization of the performance of PSCs can be achieved through interfacial engineering, which allows the tuning of the interfacial processes. Since charge recombination plays an important role in controlling the magnitude of FF and V_{OC}, ongoing research efforts should concentrate on the search for suitable interlayers between perovskites and selective contacts. So far, the reported values for FF and V_{OC} are quite close to the theoretical limit values; however, improvement in the J_{SC} value can be a new direction. The ligand-chemistry-dependent nature of the interfacial agents at the perovskite/hole transport layer junction plays a key role in the charge transport/extraction. The passivation of the $FAPbI_3$ surface reduces the non-radiative losses and suppresses ion migration in PSCs,[70–72] and can be made through the application of surface passivation agent atop of the perovskite layers. Pure $FAPbI_3$ composition has not been very effective in improving the J_{SC} value. Interfacial engineering of the perovskite absorber assists in forming high quality polycrystalline nature, possessing monolithic grains with negligible defects in the bulk compared with the surface defects. Thus, passivation of the interface can contribute towards the PCE and stable PSCs. The passivation of the $FAPbI_3$ surface with various molecules, reported so far, includes the Lewis acid–base adduct approach to produce a high-quality perovskite layer.[73] It is known that the non-bonding pair of electrons in the Lewis base are shown to be coordinated with the under/coordinated Pb^{2+} or I vacancies to form a Lewis adduct. The use of phenylalkylamines to passivate the $FAPbI_3$ surface that improves the moisture resistance, while simultaneously enhancing the electronic properties, was reported.[74] The champion PSC passivated by benzylamine exhibited a PCE of 19.2% and a V_{OC} of 1.12 V (Fig. 6). The device also retained stability up to >2800 h air exposure. Surface passivation by sulphur containing thiophenes and nitrogen containing pyridine compounds is widely exploited due to their ability to form coordination bonds with the under-coordinated Pb ions in perovskites. Improvements were also registered by using

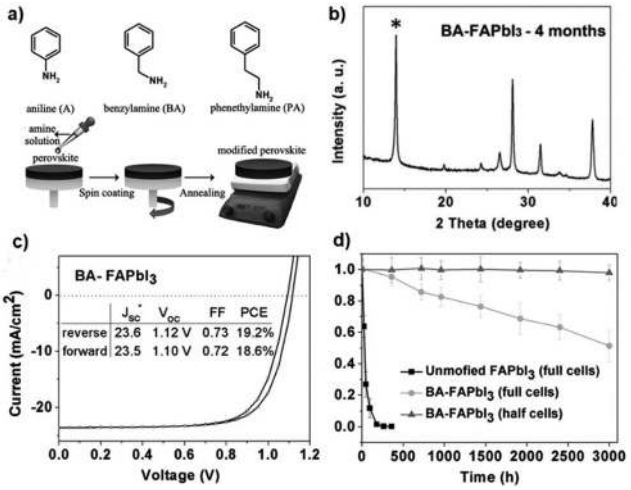

Fig. 6 (a) Chemical structures of aniline, benzylamine and phenethylamine. (b) XRD pattern of the modified BA-$FAPbI_3$ film exposed to moisture air (about 50% RH). (c) *J–V* curves of the BA-$FAPbI_3$ solar cell. (d) Moisture stability curve of unmodified $FAPbI_3$ and BA-$FAPbI_3$ on exposure to air. Reproduce with permission ref. 79 Copyright 2016, Wiley.

interfacial layers of chromium, MoO_X and PCBM, which supress metal migration.[75,76]

Recent efforts allowed us to replace the well-exploited TiO_2 with ZnO_x and SnO_x, as electron transport materials, to tap the benefits of their higher electron mobility and favourable band alignment with the perovskite layer.[77] Preliminary results of utilizing surface modifications of the TiO_2 layer with organic and inorganic passivation will allow us to direct the research to develop new electron selective contacts.[77,78] For hole transporting materials (HTMs), various competitive materials were designed and integrated in PSCs to achieve high performance. The classical Spiro-OMeTAD performs well in terms of efficiency; however, the long-term performance of the device is compromised by the usage of the ionic dopant and additives such as lithium salt (LiTFSI), *t*-butyl pyridine (*t*-BP) and/or cobalt complex. The dopant used in the HTM can migrate and the intercalation of Li^+ in the perovskite layer accelerates device degradation.[80] Organic semiconductors based on small molecules or polymers, organo-metallic compounds, and inorganic p-type semiconductors, are being investigated to substitute Spiro-OMeTAD. Small molecules offer the choice of molecular engineering of the building blocks to tune the semiconducting properties. HTMs based on cores such as triazatruxene, thiophene, and carbocyclic moieties have been explored and exhibited high performance in PSCs.[86–88] The pyridine based HTM acts as a Lewis base and offers synergistic effect for it to passivate the defects on the perovskite surface along with hole transportation.[81]

2.4 Advanced perovskite processing methods

Although the conventional precursor solution synthesized through the dissolution of high-grade precursors (PbI_2, FAI, *etc.*) in organic toxic solvents has been widely employed to acquire superior device performance, the reproducibility and cost-competitiveness were highly compromised. To overcome these challenges, the application

of pre-synthesized halide perovskite powder as precursor is emerging recently which scores with its higher reproducibility and adaptability of both wet and dryprocessibility.[82–84] Similar to the field of ceramics and metals;[85] various techniques such as mechanochemical, precipitation, and sonochemical processes can be utilised for the synthesis of the powder. δ-$FAPbI_3$ powder was synthesized using a room-temperature precipitation technique and the PSCs gave a higher reproducibility and a low trap density along with the improved efficiency as compared to the conventional route.[82,83] Followed by this, we reported Cs amalgamated δ-$Cs_{0.1}FA_{0.9}PbI_3$ powder from low-grade PbI_2. Remarkably the fabricated PSs thereof, where the double cation based absorber layer was annealed at low temperature (80 °C), showed reduced hysteresis and on par performance.[84] We propose the powder precursor route as one of the future directions for $FAPbI_3$ based PSCs. Much efforts are needed to find the extend of incorporating dopants and passivating materials into the powder. The proposed processing techniques has both advantages and disadvantages. Mechanochemical route, which is solvent free will produce highly stable perovskites at the expense of high cost of equipment and possibility for contamination from its abrasions. While the recrystallization possibility in the precipitation method will reduce the cost of powder synthesis through the use of low-grade precursors along with controlled morphological homogeneity, the requirement of large volume of solvents and stoichiometric balancing will be challenging. However, the powder precursor will open the wide possibilities of utilization of wet-fabrication techniques such as dispersion and dissolution along with the dry-fabrication techniques such as physical vapour deposition and aerosol deposition methods. Additionally, the monocrystalline perovskite-based PSCs can be an attractive direction to address environmental instability. Recent reports have revealed an exceptionally long charge carrier diffusion length (>10 μm), low trap density (10^9–10^{10} cm^{-3}), high charge mobility and low band gap for $MAPbI_3$ single crystal perovskites as compared to their polycrystalline counterparts.[86,87] The device performance showed an unparalleled enhancement from 5.49% in 2016 to 21.09% in 2019.[88,89] The current focus needs to turn from the $MAPbI_3$ based single crystal perovskite to the promising $FAPbI_3$ perovskite. Most importantly, large area PSCs are a pre-requisite for their commercialisation. Besides, the conventional laboratory techniques such as spin coating and chemical vapour deposition, new cost-effective, user-friendly, and reproducible techniques need to be employed to fabricate high quality large area $FAPbI_3$ thin films to step-up from the laboratory setup. There are reports in the literature on large area thin films fabricated through blade coating, slot-die coating, inject printing and spray coating.[90–92] All these techniques are solution based which will retain the cost-effectiveness of device fabrication. Among the four methods mentioned above, blade coating is the least inexpensive way to fabricate large area thin films along with an additional advantage of a monocrystalline structure.[93] In slot-die coating, a die is designed to have a thin channel to spread the perovskite ink to a flexible substrate.[94] Inject printing is a material efficient and contactless technique where a pressure pulse generated by a piezoelectric transducer in the continuous fluid supply controls the ejection of ink droplets on to a moving substrate.[95] Moreover, spray coating has also been used for the fabrication of perovskite layers, and this can be adapted as a future tool for the fabrication of large area PSCs due to its wide atomisation possibilities.[96] However, most of the large area PSCs fabricated till now are focussed on MA rich perovskites and attention on FA rich perovskites will accelerate enhancement in device performance and outdoor applications.

2.5 Device kinetics and understanding

A synergistic approach that can ensure the fabrication of a stable yet efficient perovskite layer can be achieved by screening new perovskite materials and their designing, to validate relationships between microstructure, phase purity, dimensionality, charge transport and device stability in a holistic manner. In this context, the development of structural characterization techniques having superior spatial resolution will enable us to visualize the perovskite degradation processes and pursue *in situ* under operando conditions. The induced structural changes and their influence should be analysed using electro-optical techniques. This will unravel the real time monitoring of charge dynamics at the nanometre scale under operational conditions. This information will establish the co-relationship between the nanostructure and the physical properties, essential for advancing the design of new materials and interfaces. Research groups are studying techniques such as *in situ* grazing-incidence small-angle neutron scattering (GISANS) to gain information about the water uptake,[97] grazing-incidence wide-angle X-ray scattering (GIWAXS) to track moisture- and heat-induced structural changes,[98–101] time-of-flight secondary-ion mass spectrometry (ToF-SIMS) to measure the ion distribution and migration during the decomposition,[102–104] *in situ* high resolution X-ray photoelectron spectroscopy (HR-XPS) to analyze thermal degradation induced compositional changes at the surface,[104] *in situ* point-resolved valence electron energy loss spectroscopy (VEELS) to understand the chemistry of the perovskite during thermal degradation[105] and *in situ* high resolution transmission electron microscopy (HR-TEM)[106] coupled with their fast Fourier transforms (FFTs),[107] selected area electron diffraction (SAED)[108] and energy dispersive X-ray analysis (EDX)[109] to visualize the microstructural variations during heat-, moisture- and electric stress-induced degradation of different perovskites and complete devices. In this direction, $FAPbI_3$ requires a more detailed study in order to grab the real information on composition–microstructure–property–performance relationships under its operando conditions. On the other hand, most of the studies on factors affecting the stability and device performances were monitored on the thin films of $FAPbI_3$ and the role of precursor solution has rarely been investigated. In a recent report, Pang *et al.* investigated the aging of the $FAPbI_3$ precursor solution and reported a deprotonation induced degradation of FAI to *s*-triazine (Scheme 2).[110] Nucleophilic amino group in FA° generated through the deprotonation of FAI undergoes addition–elimination reactions to form *s*-triazine with the removal of NH_3. The authors noted the addition of boronic derivatives with a vacant boron orbital can inhibit the deprotonation step and thereby the FAI degradation through its strong interaction with lone pair of electrons in I^-. This observation highlights the need of in-depth and real time understanding of

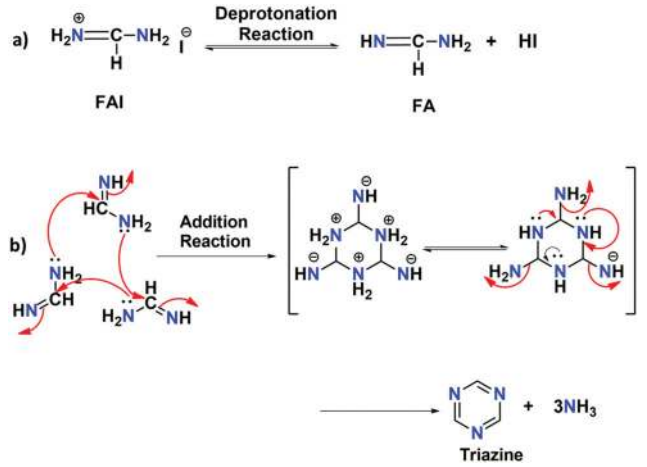

Scheme 2 Proposed degradation reaction steps of FAI in precursor solution upon aging (a) deprotonation of FAI and (b) addition–elimination reaction between FA° molecules to form *s*-triazine. Reproduced with permission from ref. 110. Copyright 2021, Wiley.

underlying reactions and mechanisms taking place throughout the process, *i.e.*, the quality of the precursor materials for the evaluation of fabricated PSCs.

3. Prerequisite of unified protocols

Reliability of PSCs is a predominant research direction for the uniform reporting of testing conditions and for this, standardized stress testing conditions will play a crucial role in substantiating the research. Environmental stress conditions to assess the long-term durability in the temperature range from −20 to 85 °C including external factors such as irradiance and humidity is important. In the absence of a unified protocol and degree of conditions used to investigate the devices under stress, it is unreasonable to draw a rational comparison for stability improvements among scientific labs reporting either innovative chemistry or new process protocols. Degradation induced by light irradiance/soaking at elevated temperatures testing should be performed firstly, and secondly, the reporting of steady-state PCEs, which is significantly different from the maximum power point, obtained from the *J*–*V* curves due to the presence of the hysteresis behavior in imprecise devices through *J*–*V* scanning. In this context, accelerated environmental stress test and performance characterization methods to probe the stability, adoption of international standards protocol that is designed for silicon or thin film based photovoltaics (IEC 61215)[111] need to be put in action for module or mini module type device testing. For lab scale devices, the initial testing should be reported exceeding 1000 hours under light soaking conditions at an elevated temperature for any investigation focused on stability enhancement. Addressing the stability challenges is paramount for the transfer of PSC technology from the lab to fab, by validating a standard testing protocol for long-term stability. For this, the nature of the organic component and the ionic characteristics must be investigated in depth, in order to achieve long-term durability, by monitoring operational stability conducted at the maximum power point tracking under continuous light illumination. Furthermore, the substitution of environmentally unfriendly and toxic lead is a daunting but an essential task. Although lead can be recycled or reused to minimize its pollution or employed for other applications, the presence of ppm amounts of lead in our body has shown neurotoxicity.

4. Future adaptability

The following measures will allow the performance of $FAPbI_3$ based PSCs and their adaptability to improve further (Fig. 7).

(i) Engineering of $FAPbI_3$ to extend light absorption, crystal optimization and processing conditions to control the formation of defect-free, segregation-free, strain-free perovskite layers. A large quantity of presynthesized $FAPbI_3$ powder will provide easy processability and reproducibility.

(ii) Designing innovative charge selective contacts, which are cost effective and easy to synthesize (inorganic as well as organic), to allow the tailoring of interfaces for enhanced charge extraction and stability improvement.

(iii) Elucidating the basic understanding of the underlying process and kinetics through real-time *in situ* characterisation studies to allow materials' optimization and interface tailoring.

(iv) New processing techniques for scaling up modules and development in a phased manner (30×30 cm^2–100×100 cm^2), which represent uniform, pin-hole free layers and precise control over thickness.

(v) Efficiency in excess of 18–20% at the module level, and increasing the aperture area to maximize device efficiency and FF.

(vi) Optimized processing techniques (slot die, blade coating, chemical bath deposition and printing) to achieve reproducibility through a wet chemistry route for the deposition of different charge selective layers.

(vii) Accelerated ageing test to validate the long-term (20+ years) performance in accordance with the IEC-61215 test conditions is required.

(viii) Outdoor testing and correlation of characteristics with accelerated ageing tests for lifetime prediction.

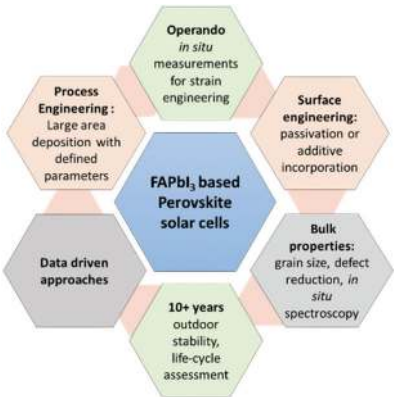

Fig. 7 Required merits for $FAPbI_3$ based perovskite solar cells.

(ix) For solar value chain, life-cycle assessment, energy-payback time evaluation and negative environmental impact valuation are required.

The development of emerging PV technology that can improve the competitiveness and dispatchability in the energy mix will allow energy transition to take place at a faster rate.

Conflicts of interest

There are no conflicts to declare.

Acknowledgements

This work was supported by the H2020 European Research Council Grant (MOLEMAT, 726360), which is gratefully acknowledged.

Notes and references

1 T. Ishihara and P. Sofronis, *Sci. Technol. Adv. Mater.*, 2018, **19**, 484–485.
2 P. K. Nayak, S. Mahesh, H. J. Snaith and D. Cahen, *Nat. Rev. Mater.*, 2019, **4**, 269–285.
3 A. Kojima, K. Teshima, Y. Shirai and T. Miyasaka, *J. Am. Chem. Soc.*, 2009, **131**, 6050–6051.
4 L. Caliò, S. Kazim, M. Grätzel and S. Ahmad, *Angew. Chem., Int. Ed.*, 2016, **55**, 14522–14545.
5 https://www.nrel.gov/pv/cell-efficiency.html, n.d.
6 W. Li, Z. Wang, F. Deschler, S. Gao, R. H. Friend and A. K. Cheetham, *Nat. Rev. Mater.*, 2017, **2**, 16099.
7 S. Kazim, M. K. Nazeeruddin, M. Grätzel and S. Ahmad, *Angew. Chem., Int. Ed.*, 2014, **53**, 2812–2814.
8 V. M. Goldschmidt, *Die Naturwissenschaften*, 1926, **14**, 477–485.
9 Z. Yi, N. H. Ladi, X. Shai, H. Li, Y. Shen and M. Wang, *Nanoscale Adv.*, 2019, **1**, 1276–1289.
10 M. R. Filip, G. E. Eperon, H. J. Snaith and F. Giustino, *Nat. Commun.*, 2014, **5**, 5757.
11 J. S. Manser, M. I. Saidaminov, J. A. Christians, O. M. Bakr and P. V. Kamat, *Acc. Chem. Res.*, 2016, **49**, 330–338.
12 E. J. Juarez-Perez, L. K. Ono, I. Uriarte, E. J. Cocinero and Y. Qi, *ACS Appl. Mater. Interfaces*, 2019, **11**, 12586–12593.
13 G. Abdelmageed, L. Jewell, K. Hellier, L. Seymour, B. Luo, F. Bridges, J. Z. Zhang and S. Carter, *Appl. Phys. Lett.*, 2016, **109**, 233905.
14 T. M. Koh, K. Fu, Y. Fang, S. Chen, T. C. Sum, N. Mathews, S. G. Mhaisalkar, P. P. Boix and T. Baikie, *J. Phys. Chem. C*, 2014, **118**, 16458–16462.
15 G. E. Eperon, S. D. Stranks, C. Menelaou, M. B. Johnston, L. M. Herz and H. J. Snaith, *Energy Environ. Sci.*, 2014, **7**, 982–988.
16 E. J. Juarez-Perez, L. K. Ono and Y. Qi, *J. Mater. Chem. A*, 2019, **7**, 16912–16919.
17 E. G. Moloney, V. Yeddu and M. I. Saidaminov, *ACS Mater. Lett.*, 2020, **2**, 1495–1508.
18 N. Rolston, K. A. Bush, A. D. Printz, A. Gold-Parker, Y. Ding, M. F. Toney, M. D. McGehee and R. H. Dauskardt, *Adv. Energy Mater.*, 2018, **8**, 1802139.
19 C. Zhu, X. Niu, Y. Fu, N. Li, C. Hu, Y. Chen, X. He, G. Na, P. Liu, H. Zai, Y. Ge, Y. Lu, X. Ke, Y. Bai, S. Yang, P. Chen, Y. Li, M. Sui, L. Zhang, H. Zhou and Q. Chen, *Nat. Commun.*, 2019, **10**, 815.
20 G. Kim, H. Min, K. S. Lee, D. Y. Lee, S. M. Yoon and S. il Seok, *Science*, 2020, **370**, 108–112.
21 L. Gu, D. Li, L. Chao, H. Dong, W. Hui, T. Niu, C. Ran, Y. Xia, L. Song, Y. Chen and W. Huang, *Sol. RRL*, 2021, 2000672.
22 T. J. McMahon, *Prog. Photovoltaics*, 2004, **12**, 235–248.
23 Y. Zhou, Z. Zhou, M. Chen, Y. Zong, J. Huang, S. Pang and N. P. Padture, *J. Mater. Chem. A*, 2016, **4**, 17623–17635.
24 G. Grancini and M. K. Nazeeruddin, *Nat. Rev. Mater.*, 2019, **4**, 4–22.
25 D. Thrithamarassery Gangadharan and D. Ma, *Energy Environ. Sci.*, 2019, **12**, 2860–2889.
26 S. Tang, S. Huang, G. J. Wilson and A. Ho-Baillie, *Trends Chem.*, 2020, **2**, 587–682.
27 A. K. Jena, A. Kulkarni and T. Miyasaka, *Chem. Rev.*, 2019, **119**, 3036–3103.
28 M. Saliba, T. Matsui, K. Domanski, J.-Y. Seo, A. Ummadisingu, S. M. Zakeeruddin, J.-P. Correa-Baena, W. R. Tress, A. Abate, A. Hagfeldt and M. Gratzel, *Science*, 2016, **354**, 206–209.
29 N. Pellet, P. Gao, G. Gregori, T.-Y. Yang, M. K. Nazeeruddin, J. Maier and M. Grätzel, *Angew. Chem., Int. Ed.*, 2014, **53**, 3151–3157.
30 W.-J. Yin, T. Shi and Y. Yan, *Appl. Phys. Lett.*, 2014, **104**, 063903.
31 S.-H. Turren-Cruz, A. Hagfeldt and M. Saliba, *Science*, 2018, **362**, 449–453.
32 T. M. Koh, K. Fu, Y. Fang, S. Chen, T. C. Sum, N. Mathews, S. G. Mhaisalkar, P. P. Boix and T. Baikie, *J. Phys. Chem. C*, 2014, **118**, 16458–16462.
33 O. A. Syzgantseva, M. Saliba, M. Grätzel and U. Rothlisberger, *J. Phys. Chem. Lett.*, 2017, **8**, 1191–1196.
34 A. Binek, F. C. Hanusch, P. Docampo and T. Bein, *J. Phys. Chem. Lett.*, 2015, **6**, 1249–1253.
35 H. Min, G. Kim, M. J. Paik, S. Lee, W. S. Yang, M. Jung and S. il Seok, *Adv. Energy Mater.*, 2019, **9**, 1803476.
36 X. Wang, Y. Fan, L. Wang, C. Chen, Z. Li, R. Liu, H. Meng, Z. Shao, X. Du, H. Zhang, G. Cui and S. Pang, *Chem*, 2020, **6**, 1369–1378.
37 J.-W. Lee, D.-H. Kim, H.-S. Kim, S.-W. Seo, S. M. Cho and N.-G. Park, *Adv. Energy Mater.*, 2015, **5**, 1501310.
38 D. J. Kubicki, D. Prochowicz, A. Hofstetter, S. M. Zakeeruddin, M. Grätzel and L. Emsley, *J. Am. Chem. Soc.*, 2017, **139**, 14173–14180.
39 Z. Peng, Q. Wei, H. Chen, Y. Liu, F. Wang, X. Jiang, W. Liu, W. Zhou, S. Ling and Z. Ning, *Cell Rep. Phys. Sci.*, 2020, **1**, 100224.
40 T. Chen, B. J. Foley, C. Park, C. M. Brown, L. W. Harriger, J. Lee, J. Ruff, M. Yoon, J. J. Choi and S.-H. Lee, *Sci. Adv.*, 2016, **2**, e1601650.

41 C. Yi, J. Luo, S. Meloni, A. Boziki, N. Ashari-Astani, C. Grätzel, S. M. Zakeeruddin, U. Röthlisberger and M. Grätzel, *Energy Environ. Sci.*, 2016, **9**, 656–662.
42 J.-P. Correa-Baena, Y. Luo, T. M. Brenner, J. Snaider, S. Sun, X. Li, M. A. Jensen, N. T. P. Hartono, L. Nienhaus, S. Wieghold, J. R. Poindexter, S. Wang, Y. S. Meng, T. Wang, B. Lai, M. V. Holt, Z. Cai, M. G. Bawendi, L. Huang, T. Buonassisi and D. P. Fenning, *Science*, 2019, **363**, 627–631.
43 A. Bercegol, F. J. Ramos, A. Rebai, T. Guillemot, J.-B. Puel, J.-F. Guillemoles, D. Ory, J. Rousset and L. Lombez, *J. Phys. Chem. C*, 2018, **122**, 23345–23351.
44 Y. Jiang, M. R. Leyden, L. Qiu, S. Wang, L. K. Ono, Z. Wu, E. J. Juarez-Perez and Y. Qi, *Adv. Funct. Mater.*, 2018, **28**, 1703835.
45 L. Luo, Y. Zhang, N. Chai, X. Deng, J. Zhong, F. Huang, Y. Peng, Z. Ku and Y.-B. Cheng, *J. Mater. Chem. A*, 2018, **6**, 21143–21148.
46 X. Zheng, C. Wu, S. K. Jha, Z. Li, K. Zhu and S. Priya, *ACS Energy Lett.*, 2016, **1**, 1014–1020.
47 J.-W. Lee, D.-H. Kim, H.-S. Kim, S.-W. Seo, S. M. Cho and N.-G. Park, *Adv. Energy Mater.*, 2015, **5**, 1501310.
48 Y. Li, J. V. Milić, A. Ummadisingu, J.-Y. Seo, J.-H. Im, H.-S. Kim, Y. Liu, M. I. Dar, S. M. Zakeeruddin, P. Wang, A. Hagfeldt and M. Grätzel, *Nano Lett.*, 2019, **19**, 150–157.
49 P. Huang, S. Kazim, M. Wang and S. Ahmad, *ACS Energy Lett.*, 2019, **4**, 2960–2974.
50 I. C. Smith, E. T. Hoke, D. Solis-Ibarra, M. D. McGehee and H. I. Karunadasa, *Angew. Chem., Int. Ed.*, 2014, **126**, 11414–11417.
51 H. Tsai, W. Nie, J.-C. Blancon, C. C. Stoumpos, R. Asadpour, B. Harutyunyan, A. J. Neukirch, R. Verduzco, J. J. Crochet, S. Tretiak, L. Pedesseau, J. Even, M. A. Alam, G. Gupta, J. Lou, P. M. Ajayan, M. J. Bedzyk, M. G. Kanatzidis and A. D. Mohite, *Nature*, 2016, **536**, 312–316.
52 H. Lai, D. Lu, Z. Xu, N. Zheng, Z. Xie and Y. Liu, *Adv. Mater.*, 2020, **32**, 2001470.
53 L. Cheng, Z. Liu, S. Li, Y. Zhai, X. Wang, Z. Qiao, Q. Xu, K. Meng, Z. Zhu and G. Chen, *Angew. Chem., Int. Ed.*, 2021, **60**, 856–864.
54 M. Pegu, M. P. U. Haris, S. Kazim and S. Ahmad, *Emergent Mater.*, 2020, **3**, 751–778.
55 S. Maheshwari, T. J. Savenije, N. Renaud and F. C. Grozema, *J. Phys. Chem. C*, 2018, **122**, 17118–17122.
56 A. O. El-Ballouli, O. M. Bakr and O. F. Mohammed, *J. Phys. Chem. Lett.*, 2020, **11**, 5705–5718.
57 Z. Wang, Y. Zhou, S. Pang, Z. Xiao, J. Zhang, W. Chai, H. Xu, Z. Liu, N. P. Padture and G. Cui, *Chem. Mater.*, 2015, **27**, 7149–7155.
58 J.-W. Lee, H.-S. Kim and N.-G. Park, *Acc. Chem. Res.*, 2016, **49**, 311–319.
59 F. Zhang and K. Zhu, *Adv. Energy Mater.*, 2020, **10**, 1902579.
60 S. Bai, P. Da, C. Li, Z. Wang, Z. Yuan, F. Fu, M. Kawecki, X. Liu, N. Sakai, J. T.-W. Wang, S. Huettner, S. Buecheler, M. Fahlman, F. Gao and H. J. Snaith, *Nature*, 2019, **571**, 245–250.
61 R. Xia, X. Gao, Y. Zhang, N. Drigo, V. I. E. Queloz, F. F. Tirani, R. Scopelliti, Z. Huang, X. Fang, S. Kinge, Z. Fei, C. Roldán-Carmona, M. K. Nazeeruddin and P. J. Dyson, *Adv. Mater.*, 2020, **32**, 2003801.
62 R. Xia, Z. Fei, N. Drigo, F. D. Bobbink, Z. Huang, R. Jasiūnas, M. Franckevičius, V. Gulbinas, M. Mensi, X. Fang, C. Roldán-Carmona, M. K. Nazeeruddin and P. J. Dyson, *Adv. Funct. Mater.*, 2019, **29**, 1902021.
63 S. Wang, Z. Li, Y. Zhang, X. Liu, J. Han, X. Li, Z. Liu, S. (Frank) Liu and W. C. H. Choy, *Adv. Funct. Mater.*, 2019, **29**, 1900417.
64 S. Akin, E. Akman and S. Sonmezoglu, *Adv. Funct. Mater.*, 2020, **30**, 2002964.
65 S. Wang, B. Yang, J. Han, Z. He, T. Li, Q. Cao, J. Yang, J. Suo, X. Li, Z. Liu, S. (Frank) Liu, C. Tang and A. Hagfeldt, *Energy Environ. Sci.*, 2020, **13**, 5068–5079.
66 J. Wang, X. Ye, Y. Wang, Z. Wang, W. Wong and C. Li, *Electrochim. Acta*, 2019, **303**, 133–139.
67 J. Zhao, Y. Deng, H. Wei, X. Zheng, Z. Yu, Y. Shao, J. E. Shield and J. Huang, *Sci. Adv.*, 2017, **3**, eaao5616.
68 T. Haeger, R. Heiderhoff and T. Riedl, *J. Mater. Chem. C*, 2020, **8**, 14289–14311.
69 C. Zhu, X. Niu, Y. Fu, N. Li, C. Hu, Y. Chen, X. He, G. Na, P. Liu, H. Zai, Y. Ge, Y. Lu, X. Ke, Y. Bai, S. Yang, P. Chen, Y. Li, M. Sui, L. Zhang, H. Zhou and Q. Chen, *Nat. Commun.*, 2019, **10**, 815.
70 J. Kim, A. Ho-Baillie and S. Huang, *Sol. RRL*, 2019, **3**, 1800302.
71 F. Gao, Y. Zhao, X. Zhang and J. You, *Adv. Energy Mater.*, 2020, **10**, 1902650.
72 E. Aydin, M. Bastiani and S. Wolf, *Adv. Mater.*, 2019, **31**, 1900428.
73 J.-W. Lee, H.-S. Kim and N.-G. Park, *Acc. Chem. Res.*, 2016, **49**, 311–319.
74 W. Luo, C. Wu, D. Wang, Y. Zhang, Z. Zhang, X. Qi, N. Zhu, X. Guo, B. Qu, L. Xiao and Z. Chen, *ACS Appl. Mater. Interfaces*, 2019, **11**, 9149–9155.
75 H. Abdy, A. Aletayeb, M. Kolahdouz and E. A. Soleimani, *AIP Adv.*, 2019, **9**, 015216.
76 C. C. Boyd, R. Cheacharoen, K. A. Bush, R. Prasanna, T. Leijtens and M. D. McGehee, *ACS Energy Lett.*, 2018, **3**, 1772–1778.
77 S. S. Shin, S. J. Lee and S. il Seok, *Adv. Funct. Mater.*, 2019, **29**, 1900455.
78 M. M. Tavakoli, P. Yadav, R. Tavakoli and J. Kong, *Adv. Energy Mater.*, 2018, **8**, 1800794.
79 F. Wang, W. Geng, Y. Zhou, H.-H. Fang, C.-J. Tong, M. A. Loi, L.-M. Liu and N. Zhao, *Adv. Mater.*, 2016, **28**, 9986–9992.
80 P. Kung, M. Li, P. Lin, Y. Chiang, C. Chan, T. Guo and P. Chen, *Adv. Mater. Interfaces*, 2018, **5**, 16490–16494.
81 B. Xu, Z. Zhu, J. Zhang, H. Liu, C.-C. Chueh, X. Li and A. K.-Y. Jen, *Adv. Energy Mater.*, 2017, **7**, 1700683.
82 Y. Zhang, S.-G. Kim, D.-K. Lee and N.-G. Park, *ChemSusChem*, 2018, **11**, 1813–1823.
83 Y. Zhang, S. Seo, S. Y. Lim, Y. Kim, S.-G. Kim, D.-K. Lee, S.-H. Lee, H. Shin, H. Cheong and N.-G. Park, *ACS Energy Lett.*, 2020, **5**, 360–366.

84 M. P. U. Haris, S. Kazim and S. Ahmad, *ACS Appl. Energy Mater.*, 2021, **4**, 2600–2606.
85 C. B. Carter and M. G. Norton, *Ceramic materials: science and engineering*, Springer, New York, 2013.
86 D. Shi, V. Adinolfi, R. Comin, M. Yuan, E. Alarousu, A. Buin, Y. Chen, S. Hoogland, A. Rothenberger, K. Katsiev, Y. Losovyj, X. Zhang, P. A. Dowben, O. F. Mohammed, E. H. Sargent and O. M. Bakr, *Science*, 2015, **347**, 519–522.
87 B. Murali, H. K. Kolli, J. Yin, R. Ketavath, O. M. Bakr and O. F. Mohammed, *ACS Mater. Lett.*, 2020, **2**, 184–214.
88 W. Peng, L. Wang, B. Murali, K.-T. Ho, A. Bera, N. Cho, C.-F. Kang, V. M. Burlakov, J. Pan, L. Sinatra, C. Ma, W. Xu, D. Shi, E. Alarousu, A. Goriely, J.-H. He, O. F. Mohammed, T. Wu and O. M. Bakr, *Adv. Mater.*, 2016, **28**, 3383–3390.
89 Z. Chen, B. Turedi, A. Y. Alsalloum, C. Yang, X. Zheng, I. Gereige, A. AlSaggaf, O. F. Mohammed and O. M. Bakr, *ACS Energy Lett.*, 2019, **4**, 1258–1259.
90 S. Lee, S. Bae, D. Kim and H. Lee, *Adv. Mater.*, 2020, **32**, 2002202.
91 J. Lee, D. Lee, D. Jeong and N. Park, *Adv. Funct. Mater.*, 2019, **29**, 1807047.
92 N.-G. Park and K. Zhu, *Nat. Rev. Mater.*, 2020, **5**, 333–350.
93 Y. Zhong, R. Munir, J. Li, M.-C. Tang, M. R. Niazi, D.-M. Smilgies, K. Zhao and A. Amassian, *ACS Energy Lett.*, 2018, **3**, 1078–1085.
94 S. Huang, C. Guan, P. Lee, H. Huang, C. Li, Y. Huang and W. Su, *Adv. Energy Mater.*, 2020, **10**, 2001567.
95 F. Mathies, H. Eggers, B. S. Richards, G. Hernandez-Sosa, U. Lemmer and U. W. Paetzold, *ACS Appl. Energy Mater.*, 2018, **1**, 1834–1839.
96 Q. Jiang, Y. Zhao, X. Zhang, X. Yang, Y. Chen, Z. Chu, Q. Ye, X. Li, Z. Yin and J. You, *Nat. Photonics*, 2019, **13**, 460–466.
97 J. Schlipf, L. Bießmann, L. Oesinghaus, E. Berger, E. Metwalli, J. A. Lercher, L. Porcar and P. Müller-Buschbaum, *J. Phys. Chem. Lett.*, 2018, **9**, 2015–2021.
98 J. Yang and T. L. Kelly, *Inorg. Chem.*, 2017, **56**, 92–101.
99 K. M. Fransishyn, S. Kundu and T. L. Kelly, *ACS Energy Lett.*, 2018, **3**, 2127–2133.
100 J. Yang, B. D. Siempelkamp, D. Liu and T. L. Kelly, *ACS Nano*, 2015, **9**, 1955–1963.
101 J. Yang and T. L. Kelly, *Inorg. Chem.*, 2017, **56**, 92–101.
102 D. Xu, X. Hua, S.-C. Liu, H.-W. Qiao, H.-G. Yang, Y.-T. Long and H. Tian, *Chem. Commun.*, 2018, **54**, 5434–5437.
103 K. Domanski, J.-P. Correa-Baena, N. Mine, M. K. Nazeeruddin, A. Abate, M. Saliba, W. Tress, A. Hagfeldt and M. Grätzel, *ACS Nano*, 2016, **10**, 6306–6314.
104 N.-K. Kim, Y. H. Min, S. Noh, E. Cho, G. Jeong, M. Joo, S.-W. Ahn, J. S. Lee, S. Kim, K. Ihm, H. Ahn, Y. Kang, H.-S. Lee and D. Kim, *Sci. Rep.*, 2017, **7**, 4645.
105 J. A. Aguiar, S. Wozny, T. G. Holesinger, T. Aoki, M. K. Patel, M. Yang, J. J. Berry, M. Al-Jassim, W. Zhou and K. Zhu, *Energy Environ. Sci.*, 2016, **9**, 2372–2382.
106 G. Divitini, S. Cacovich, F. Matteocci, L. Cinà, A. di Carlo and C. Ducati, *Nat. Energy*, 2016, **1**, 15012.
107 T. W. Kim, N. Shibayama, L. Cojocaru, S. Uchida, T. Kondo and H. Segawa, *Adv. Funct. Mater.*, 2018, **28**, 1804039.
108 S. Chen, X. Zhang, J. Zhao, Y. Zhang, G. Kong, Q. Li, N. Li, Y. Yu, N. Xu, J. Zhang, K. Liu, Q. Zhao, J. Cao, J. Feng, X. Li, J. Qi, D. Yu, J. Li and P. Gao, *Nat. Commun.*, 2018, **9**, 4807.
109 Y.-H. Seo, J. H. Kim, D.-H. Kim, H.-S. Chung and S.-I. Na, *Nano Energy*, 2020, **77**, 105164.
110 C. Chen, Y. Rao, Z. Li, X. Wang, G. Cui, W. Wang and S. Pang, *Sol. RRL*, 2021, 2000715.
111 P. Holzhey and M. Saliba, *J. Mater. Chem. A*, 2018, **6**, 21794–21808.

